Spectroscopic Modelling of Cold ATLASGAL Dust Clumps

Mid-Term Phase II Report

Deepak Chahal
SC18M017

Master of Science in Astronomy and Astrophysics
Supervisor: Dr. Jagadheep D.

Dept. of Earth & Space Sciences
Indian Institute of Space Science and Technology
Thiruvananthapuram, India
March 2020

1. INTRODUCTION

The primary aim of this project is to study a sample of dense clumps selected from the Hi-GAL and ATLASGAL survey which are in early stages of high mass star formation, to understand their physical properties and kinematics using molecular spectroscopy. Since different molecular transitions traces different physical properties of the clumps, this project aims to model the spectra for several molecules such as relatively low density gas tracers ^{12}CO, ^{13}CO, $C^{18}O$ and relatively high density gas tracers HCO^+, $H^{13}CO^+$, HCN and N_2H^+.

2. PHASE I – SUMMARY

JCMT data is available for 10 cold ATLASGAL dust clumps, from which one source (AG 36.899-00.409) is selected for molecular analysis. Preliminary analysis was done by discussing the theoretical methodology for the derivation of parameters such as excitation temperature, line width, column density etc. The comparison of numerical estimates of parameters was drawn from two approaches : LTE (Local Thermodynamic Equilibrium) and non-LTE. Data cubes were modelled with both LTE & non-LTE methods for CO and its isotopologues in CASSIS, which resulted in excitation temperature, LSR velocity, column density maps. The gas traced by ^{13}CO is found to be isothermal, as the temperature was uniform. Traces of molecular outflow were detected in CO spectrum, which are clearly seen in CO integrated intensity map.

3. CHARACTERIZATION OF DUST EMISSION

The characterization of dust emission in the clump was performed by downloading the data from Herschel Science Archive. Data are already processed using Herschel standard pipeline. Herschel data for five bands centered at 70, 160, 250, 350 and 500 μm, and 870 μm data from ATLASGAL survey (Schuller, 2009) were used.

3.1 Data Analysis

In order to generate dust temperature and column density maps for each pixel, a pixel-by-pixel fitting of all these six dust maps is required. But resolution and plate scale are different for different maps. So to achieve a certain pixel must correspond to same co-ordinates in sky for each map, an analysis to convolve each dust emission map was done using HIPE (Herschel Interactive Processing Environment). Units of all maps were converted to Jy/pixel using ‘ConvertImageUnit’. The plate scale and spectral resolution of each map was convolved as per 500 μm map, using the command ‘PhotometricConvolution’ in HIPE. To subtract the background emission, a region with constant dust emission is selceted and subtracted from corresponding clump region in dust emission maps.

3.2 SED Fitting

Dust emission was modelled for each pixel with modified blackbody given by :

$$S(\nu) - I_{bkg}(\nu) = \Omega\, B(\nu, T_d)\, (1 - e^{\tau})$$

where S(ν) is flux density of each pixel, I_{bkg} is estimated background, Ω is solid angle subtended by each pixel (14" ×14"), B(ν, T_d) is Planck function, T_d is dust temperature and τ is the optical depth. And the Hydrogen column density was derived from its relation with optical depth, given by :

$$\tau = \mu_{H2}\, m_H\, \kappa_\nu\, N(H_2) / R$$

where m_H is mass of the hydrogen atom, μ_{H2} is mean molecular weight, κ_ν is dust opacity, $N(H_2)$ is column density and R is gas to dust ratio which is assumed to be 100.
Fitting of the dust emission pixel by pixel was carried out using 'lmfit' tool in Python, and corresponding SED fitted plots are sown in the Fig 1.

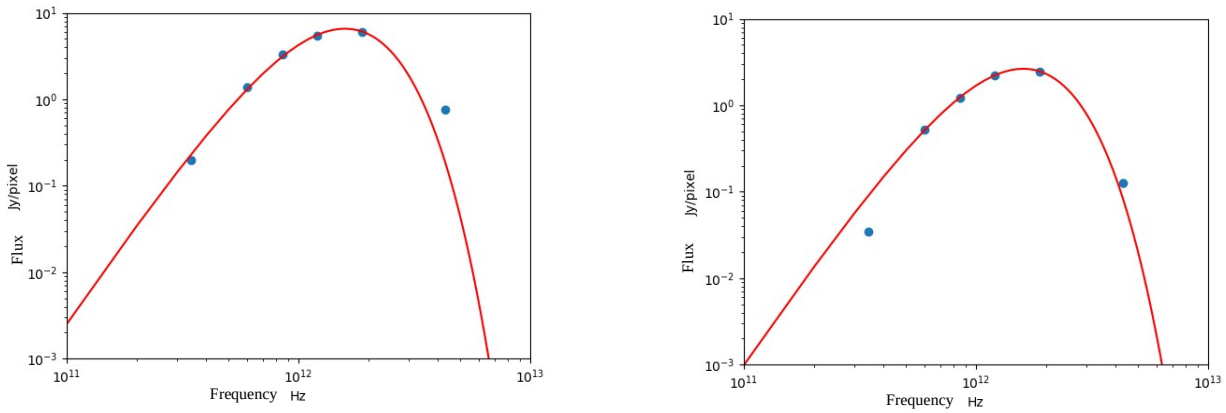

Fig 1 : SED fit for two central pixels in dust emission maps.

3.3 DISCUSSION

Dust Temperature : Temperature map estimated from SED fitting of all the pixels are shown in Fig 2. The range of temperature is found to be 14-18 K in the central region, where two core exists. While the temperature is found higher in surrounding region compare to center.

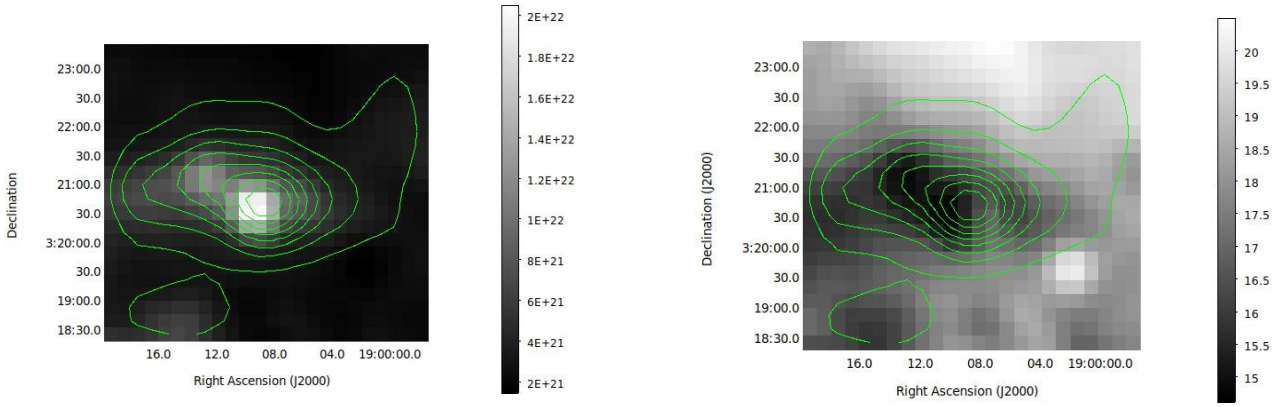

Fig 2 : SED pixel by pixel fitted maps of Column Density (left) and Dust Temperature (right) plotted with yellow contours of dust continuum emission 500 μm map.

Column Density : Hydrogen column density map estimated from SED fitting is also shown in Fig 2. The maximum hydrogen column density is observed at the center of core-1 ~ 2.07×10^{22} cm^{-2}, which ranges from 9×10^{21}- 2×10^{22} cm^{-2} around the central region.

4. HIGH DENSITY GAS TRACERS

The core properties were studied by modelling the relatively high density gas tracers such as HCN, HCO^+, CH_3OH etc. A more detailed description is mentioned in further subsections.

4.1 HCN : Hyperfine fitting

JCMT data are available for HCN J=4-3 transition, which comprises of six hyperfine lines. By modelling these all hyperfine lines together will provide an estimate of excitation temperature, optical depth and column density. Some anomalies were found in the HCN hyperfine lines as shown in Fig 3, i.e their observed relative intensity ratios are different from the theoretical intensity ratios. Similar anomalies are observed in HCN J=1-0, J=3-2 hyperfine lines in the star forming region. (Mullins, 2016; Burgk and Muders, 2004) To confirm the anomalies further, other ATLASGAL dust clumps were checked and they also found to have similar HCN J=4-3 anomalies.

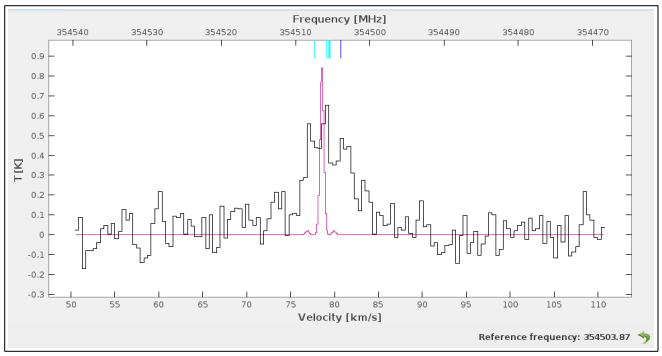

Fig 3 : HCN hyperfine data plotted with relative theoretical intensities of HCN J=4-3 hyperfine lines.

HCN spectrum was smoothed to a velocity resolution of 0.2 km/s. Since modelling of hyperfine lines is not possible in CASSIS, as it model by considering theoretical relative intensities of all hyperfine lines. Prominently three components are seen in HCN spectrum in Fig 4, so the lines were modelled by taking three separate components. The estimate of parameters were taken from the modelling results of the central component. The column density estimated from the LTE modelling is $N(HCN) \sim 5\times10^{12}\ cm^{-2}$. The corresponding abundance ratio is $X(HCN) \sim 2\times10^{-11}$, which is much lower than what is typically observed $1\times10^{-10} < X(HCN) < 1\times10^{-9}$.

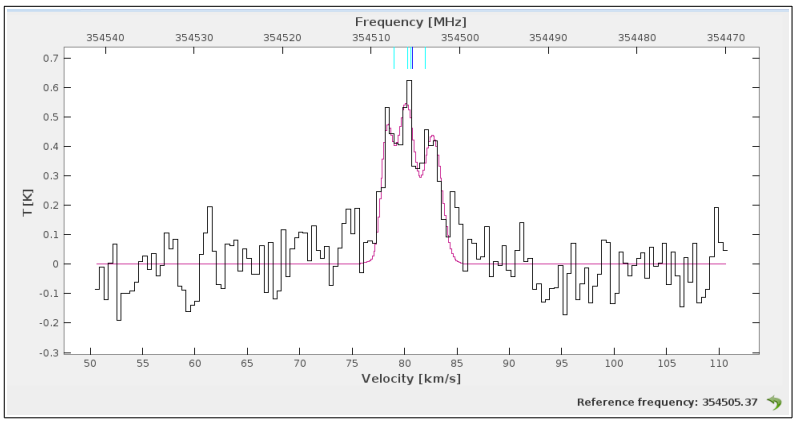

Fig 4 : A modelled spectrum of HCN by optimizing CASSIS parameters

The LTE hyperfine modelling produces lower estimates of optical depth, which in results provide a lower column density. It is also found that to model the observed main beam temperature with LTE method, the excitation temperature should be very low. So a non-LTE approach is applied for modelling the HCN spectrum. Since non-LTE model finds an optimum solution for every temperature, so an estimate of temperature is taken as 19 and 27 K which corresponds to dust and ^{13}CO temperature respectively. The column density of HCN was modelled pixel by pixel for all the central pixels as shown in Fig 5, where significant S/N is present. The estimated peak column density is N(HCN) ~ 7×10^{14} cm^{-2}, which is well within the range of typically found abundance ratio.

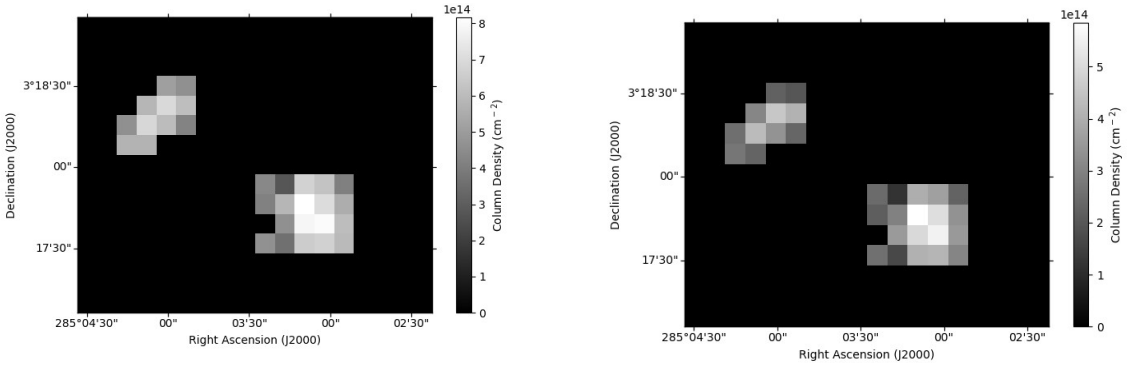

Fig 5 : HCN Column Density map modelled with constant excitation temperature 19 K (left) and 27 K (right)

4.2 HCO^+ : The Infall Tracer

In dense cloud cores, HCO^+ has a tendency to become self-absorbed. For a spherical and static cloud, emission will be symmetric about the line of sight and self-absorbed. In case of radial motion around core, emission from rear end is not absorbed as it travels through core. While the emission from front is absorbed by nearby molecular gas. So for inward radial flow, rear emission is blueshifted and front emission is redshifted, producing a blueshifted asymmetric line profile. This line profile is the predominant tool to probe infall motion in the star forming cloud cores.

JCMT data are available in the form of six maps for HCO^+ J=4-3 (Rest frequency = 356.734 MHz) transition. Two perpendicular maps are also available for $H^{13}CO^+$ J=4-3 (Rest Frequency = 346.998MHz) transition. HCO^+ spectrum was smoothed to a velocity resolution of 0.2 km/s. As expected two spectrally resolved components are clearly seen in HCO^+ spectrum, where blueshifted one is brighter than redshifted one, provides the proof of blueshifted asymmetric profile as shown in Fig 6. While S/N is very low in $H^{13}CO^+$ spectra, hardly any signal is visible even after smoothing to a velocity resolution of 0.8 km/s.

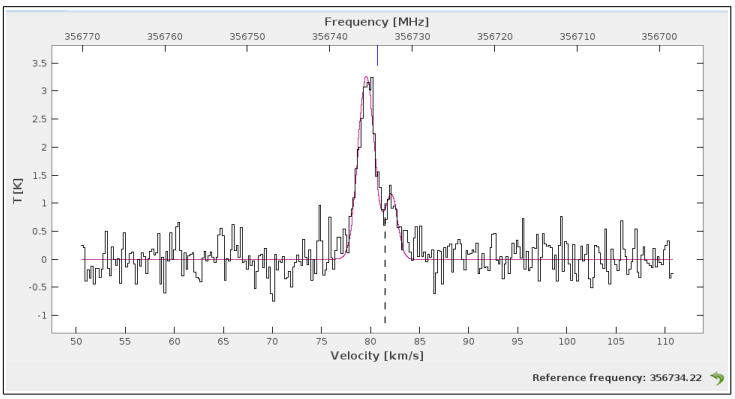

Fig 6 : HCO^+ spectrum fitted with two components : blueshifted & redshifted.

The presence of absorption is confirmed by matching the frequency of absorption festure with the frequency where $C^{18}O$ spectrum peaks. An analytical radiative transfer model is used to fit the asymmetric blueshifted self-absorbed profile and gives an estimate of infall velocity. Several radiative models are discussed in (Vries and Meyer, 2004) for the modelling of asymmertic line profile, one of the optimum model (Hillmap5) was used here. One of the fitted spectra is shown in Fig 7, and the corresponding infall velocity is 0.926 km/s.

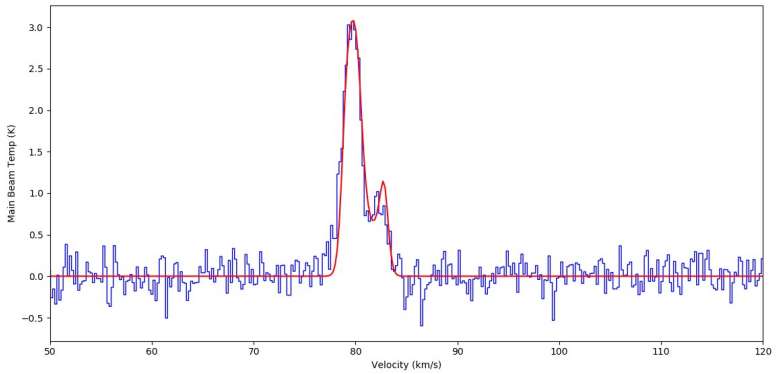

Fig 7 : HCO^+ spectrum fitted with a radiative transfer (Hillmap5) model.

4.3 CH_3OH

Single pointed observation is available for the CH_3OH J=7-6 transition, and the corresponding molecular transition contains multiple lines as shown in Fig 7. The modelling was done with LTE method in CASSIS by taking temperatures same as $C^{18}O$ and dust emission. Both of the temperature provide very low estimate of column density and an uneven fitting. So the temperature is reduced further, and an optimum fit was found at ~ 9 K as shown in Fig 8. The column density estimated to be $N(CH_3OH) \sim 1\times10^{15}\,cm^{-2}$, which is well within the range of what is typically observed. Such low temperature is due to subthermal excitation of CH_3OH gas in the core.

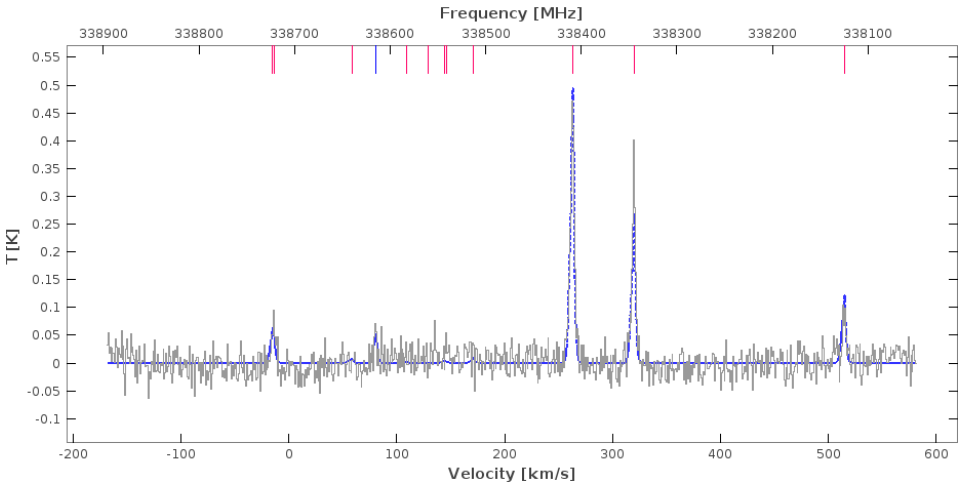

Fig 8 : A modelled spectrum of CH_3OH with LTE approach

6. Future Work

Fitting a density profile will provide an insight about the evolutionary stages of the core. So the hydrogen density estimated from dust emission is to be fitted with density profile as a function of distance from center. All the molecular analysis is just performed on one source till now, similar kind of work is required to be performed for some other sources also which are in different early stages of star formation. Both the relatively low and high gas tracers are to be modelled for each source to study their properties in a very elaborative way.

References

Schuller, F., Menten, K.M., Contreras, Y., Wyrowski, F., Schilke, P., Bronfman, L., Henning, T., Walmsley, C.M., Beuther, H., Bontemps, S. and Cesaroni, R., 2009. ATLASGAL–The APEX telescope large area survey of the galaxy at 870 m. *Astronomy & Astrophysics*, *504*(2), pp.415-427.

De Vries, C.H. and Myers, P.C., 2005. Molecular line profile fitting with analytic radiative transfer models. *The Astrophysical Journal*, *620*(2), p.800.

Mullins, A.M., Loughnane, R.M., Redman, M.P., Wiles, B., Guegan, N., Barrett, J. and Keto, E.R., 2016. Radiative transfer of HCN: interpreting observations of hyperfine anomalies. *Monthly Notices of the Royal Astronomical Society*, *459*(3), pp.2882-2892.

Schmid-Burgk, J., Muders, D., Mueller, H.S. and Brupbacher-Gatehouse, B., 2004. Hyperfine structure in HCO and CO: Measurement, analysis, and consequences for the study of dark clouds. *Astronomy & Astrophysics*, *419*(3), pp.949-964.